Chapter 5

Structural Features of the Cytochrome *c* Molten Globule Revealed by Fluorescence Energy Transfer Kinetics

*Adapted from J. G. Lyubovitsky, H. B. Gray, J. R. Winkler, *J. Am. Chem. Soc*., 124, 14840-14841 (2002)

INTRODUCTION

Partially folded states of some proteins at equilibrium were first recognized in the early 1970s.[1] Interest in these states increased when it was determined that for different proteins they share common physical properties: compactness, native-like secondary structure and lack of rigid tertiary structure. The label 'molten globule' emerged years later from work of Ogushi and Wada on salt-induced globular state of cytochrome *c* at low pH.[2]

Over the years, the label 'molten globule' has been assigned to partially folded proteins produced by a number of means: variation of the solvent conditions, removal of ligand or prosthetic group, temperature, pressure, chaperons, etc.[3] Classification of these equilibrium compact states as molten globules is usually not based on studies of their conformations but on indirect measurements of hydrophobicity and the averaged ensemble properties such as fluorescence intensity, CD and absorbance.

Today, it is generally accepted that there is a wide diversity in molten globule states. This diversity depends on the individual protein species involved and the experimental condition used to generate the molten globule state.[4] Molten globules that are somewhat ordered and retain tertiary contacts of the native state can be and have been studied by NMR.[5-7] For most molten globules, however, NMR properties are much more like unfolded proteins due to large conformational fluctuations. Extensive conformational heterogeneity and increased dynamic averaging preclude observations and any meaningful interpretations of distance-dependent nuclear Overhauser effects (NOEs),[8] rendering most molten globule states not amenable to NMR investigations.

It has been proposed that the molten globule state is a common intermediate that occurs

early in the folding pathways of globular proteins.[9] Recently, it has been suggested that in some cases molten globules correspond to late-folding intermediates.[4,10] More detailed characterization of molten globules and protein folding intermediates is necessary to clarify the relationship between the two species.

Molten Globule of Cytochrome *c*

Cytochrome *c* was the first protein in which a globular state induced by salt at low pH was named a "molten globule[2]". Goto *et al.* later demonstrated that the conformational transition from acid-unfolded protein to this globular state is mediated by anion binding.[11] The structure of the cytochrome *c* molten globule state was shown to depend strongly on the size of the added anion.[12] In addition to salts, polyols[13] and some alcohols[14,15] have been shown to stabilize the molten globule state in cytochrome *c* at low pH.

We have investigated the conformation of *Saccaromyces cerevisiae* iso-1 cytochrome *c* (cyt *c*) in its molten globule state using fluorescence energy transfer (FET) kinetics. For our experiments, we labeled the thiolate sulfur of C102 in the yeast protein with a dansyl fluorophore (DNS(C102)-cyt *c*); the DNS fluoresces intensely when the protein is unfolded, but is significantly quenched by energy transfer to the heme in compact conformations. Analysis of the fluorescence decay profiles has provided insights into the distributions of distances between donor (***D***) and acceptor (***A***) labeled residues.[16] In the Förster model, the rate of energy transfer is equal to the decay rate of the unquenched fluorophore (k_o) when the ***D-A*** distance is equal to the critical length (r_0). Under typical conditions, FET rates can be measured for ***D-A*** distances in the range $0.3\ r_0 \leq r \leq 1.5\ r_0$. The critical length ($r_0$) of the DNS-heme FET pair is 40 Å, meaning that a 12-60 Å ***D-A*** distance range can be probed in

the modified protein. Unlike other probes that report on the average properties of the ensemble (fluorescence intensity, CD, X ray scattering, absorbance), FET kinetics reveal the conformational heterogeneity of the polypeptide.[17,18]

MATERIALS AND METHODS

The materials and methods relevant to this chapter are described in the corresponding section of Chapter 2. Those introduced in this chapter are described below.

Circular Dichroism

Circular dichroism data were acquired using an Aviv Model 62ADS spectropolarimeter equipped with a thermostated sample holder. Spectra were collected at 22°C unless specified. Buffers used were: 0.05 M sodium phosphate, pH 7 for the native protein; H_2SO_4, pH ~ 2 for the acid-unfolded state; 0.7–1 M Na_2SO_4/H_2SO_4, pH ~2 for the molten globule state.

Thermal Denaturation

For the thermal unfolding transition of the DNS(C102)-cyt *c* molten globule, the ellipticity at 222 nm was recorded from –1°C to 80°C at 1°C intervals (0.7 M Na_2SO_4/H_2SO_4, pH ~2, [DNS(C102)-cyt *c*] = 2.0 – 10.0 μM). The time between successive data points was about 8 min. Reversibility was confirmed by running the reaction in reverse back to the initial temperature or by cooling the sample to the initial temperature, revisiting a few data points, and comparing the ellipticity to the prior value.

Small-Angle X-ray Scattering (SAXS)

SAXS measurements were made using the Beam Line 4-2 at the Stanford Synchrotron Radiation Laboratory.[19-21] The sample cell used was 15 μL in volume with mica windows. It was kept at 23°C by circulating temperature-controlled water. The scattering data were collected on folded, molten globule and acid-unfolded C102S variant of yeast iso-1 cytochrome *c*; folded and acid-unfolded DNS(C102)-cyt *c*. Severe aggregation of DNS(C102)-cyt *c* molten globule at concentrations required for SAX experiments precluded the measurements. The data was processed with programs SAPOKO and OTOKO. Radii of gyration were estimated from Guinier analysis[22]

$$\ln(I(S)) = \ln(I(0) - \frac{4\pi^2 R_g^2}{3} S^2$$

where R_g = radius of gyration, S = (2sinθ)/λ, 2θ = scattering angle, and λ = X-ray wavelength. The radius of gyration was determined from a Guinier plot for each concentration and extrapolated to zero concentration by plotting R_g versus concentration as shown in **Figure 5.6**.

Fluorescence Decay Kinetics

Fluorescence decay measurements were performed using the third harmonic of regeneratively amplified, mode-locked Nd-YAG laser (355 nm, 50 ps, 0.5 mJ) for excitation and a picosecond streak camera (Hamamatsu C5680) for detection. Magic-angle excitation and collection conditions were employed throughout. DNS fluorescence was selected with a long-pass cutoff filter (>430 nm). The C5680 was used in photon counting mode. Data were collected at several protein concentrations (300 nM to 3 μM) to check for aggregation and

was analyzed as described in Ref. 18 and Chapter 2.

RESULTS AND DISCUSSION

Circular Dichroism

As expected, the molten globule has very similar helix content to the native state, whereas the acid-denatured protein exhibits no secondary structure (**Figure 5.1**). The CD spectrum in the aromatic region (260-300 nm) shows two sharp peaks (282 and 290 nm) from tryptophan and/or tyrosine[23] for the native state; it is featureless for both the acid-denatured (pH 2)

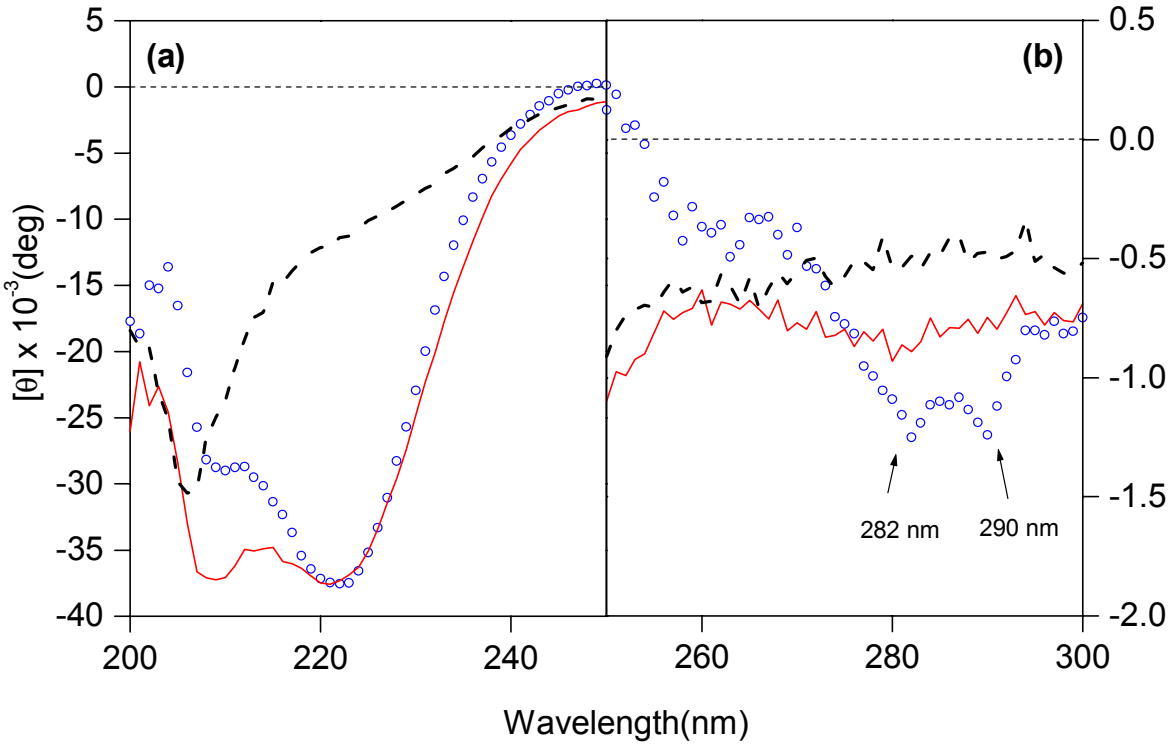

Figure 5.1. (a) Far- and (b) near-UV CD spectra of DNS(C102)-cyt *c* at 22°C. (—) the native state, (o) molten globule state, and acid-denatured state (- -).

protein and the molten globule ($[SO_4^{2-}]$ > 0.7 M), indicating the absence of tertiary structure.[24]

Absorption Spectroscopy

In the native state, the heme in DNS(C102)-cyt *c* is low-spin with Met80/His18 axial coordination. The Soret band is centered at 410 nm, and the Met80→Fe(III) charge-transfer transition is clearly visible at 695 nm (**Figure 5.2**). In the acid-denatured state, the protein is high-spin, that is, neither Met80 nor His18 is coordinated; [25-27] both the Q-bands and the Soret absorption blue shift from their positions in the native state. The Soret is centered at 396 nm, and there is a band at 620 nm attributable to an electronic transition in a high-spin heme.[28] The Soret band is centered at 400 nm in the spectrum of the molten globule, and the

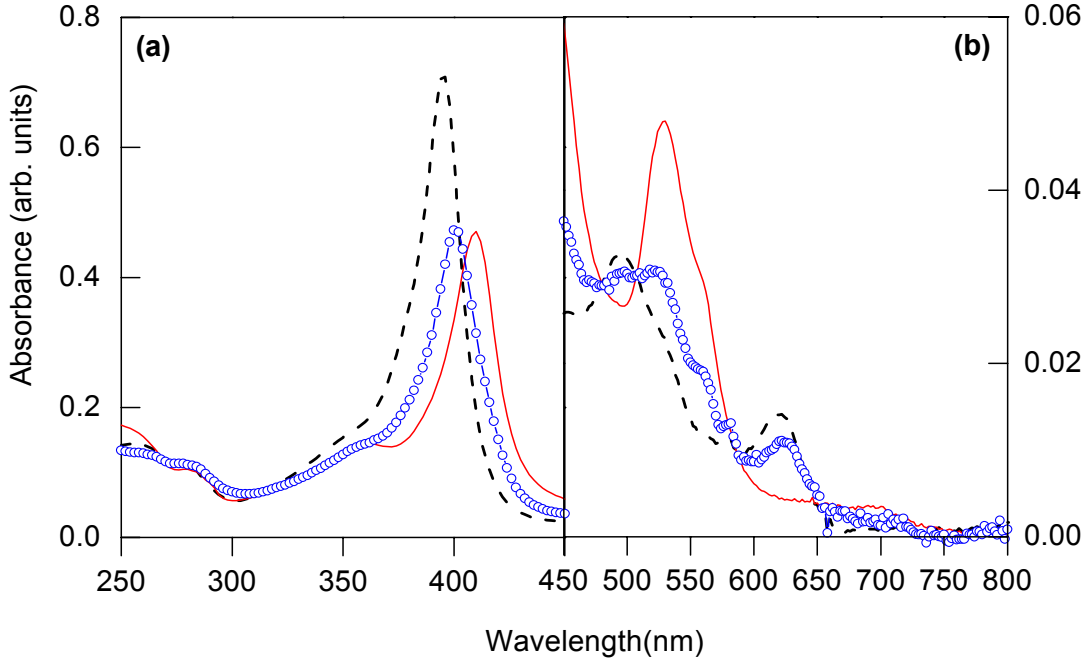

Figure 5.2. (a) Soret and (b) Q-band absorption spectra of DNS(C102)-cyt *c* at 22°C. (—) pH 7 native state, (o) molten globule state, and acid-unfolded state (- -).

Q-bands red shift relative to their positions in the acid-denatured protein. The heme in the cyt *c* molten globule is believed to be mixed spin, with His18 coordinated to iron in both spin states; Met80 is coordinated in the low-spin species, but not in the high-spin state.[24-26,29]

Thermal Denaturation

Far-UV CD spectra show that the thermal unfolding transition of the DNS(C102)-cyt *c* molten globule at pH 2 is cooperative (**Figure 5.3**). The 309 K midpoint temperature (T_m) is in excellent agreement with that previously observed for the thermal unfolding

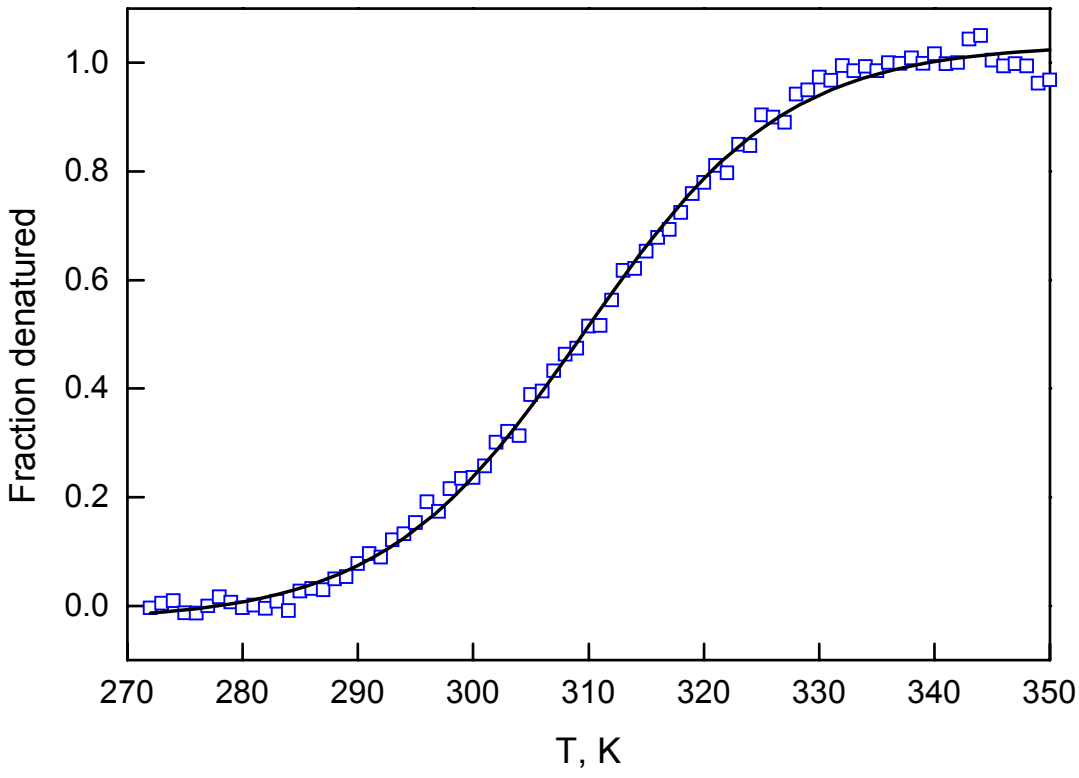

Figure 5.3. Plot of fraction denatured versus temperature for the A↔D transition of DNS(C102)-cyt *c* (0.7 M Na_2SO_4/H_2SO_4, pH 2).

transition of the cyt *c* (C102T mutant) molten globule.[30] The transition in DNS(C102)-cyt *c* is more than 90% reversible. The thermal unfolding transition of the molten globule of C102S mutant, (0.33 M Na_2SO_4/H_2SO_4, pH 2, data not shown) however, showed somewhat more cooperativity.

Small-Angle X-ray Scattering (SAXS)

The SAXS method is sensitive to size, compactness and shape of a scattering macromolecule. The scattering intensity from a protein in solution, however, is low due to a competing scattering from the solvent. It is on the order of 10% of what the scattering from a protein would be in vacuo.[21] Hence SAXS measurements on small proteins require large quantities of protein with concentrations of proteins on the scale of 0.5 mM per sample. These high protein concentrations frequently lead to aggregation, in addition to radiation-induced damage and radiation-induced aggregation, which render SAXS measurements not possible for many proteins.

Typical experimental SAXS patterns for native state (pH 7) and acid-unfolded state (pH 2) of cytochrome *c* (yeast iso-1 variant) are shown in **Figure 5.4**. The difference in the scattering by native (globular) state and unfolded (coil-like state) is further highlighted in the Kratky plots (Figure 5). Globular proteins scatter as S^{-4} at high S values (0.02 –0.04 Å) while random coil scatters as S^{-1}.[20] Thus, the Kratky plot for a random coil is proportional to S^1 and to S^{-2} for a globular protein. For a globular protein, therefore, the Kratky plot has a peak. The position of the peak depends on the radius of gyration (R_g).[31] **Figure 5.5** clearly shows that pH 7 native state and pH 2 salt-induced molten globule state of cytochrome *c*

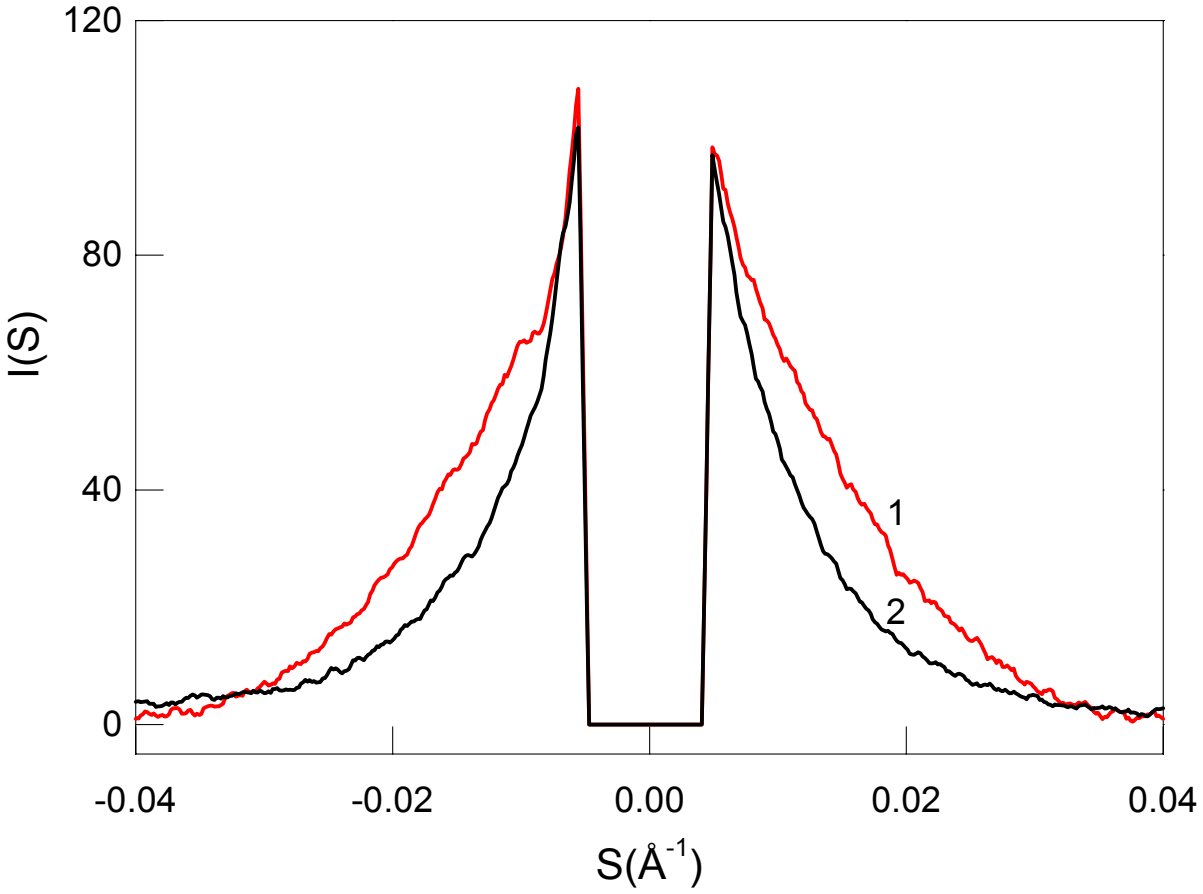

Figure 5.4. Synchrotron SAXS patterns for the pH 7 native (1) and pH 2 acid-unfolded (2) yeast iso-1 cytochrome *c*.

(yeast iso-1 variant) are globular while pH 2 acid-unfolded state is in a Gaussian chain-like conformation. The peak maximum for the molten globule state occurs at a lower S than for the native state, indicating a larger radius of gyration.

Radii of gyration for folded, salt-induced molten globule, and acid-unfolded cytochrome *c* are (yeast iso-1 variant) summarized in **Table 5.1**. Radii of gyration for horse heart

cytochrome *c*[31] are included for comparison. As seen, within the error of the SAXS experiment, (± 2 Å), the radii of gyration are essentially identical for the yeast iso-1 and horse heart cytochrome *c* in the respective conformations.

Table 5.1. Radii of gyration for *S. cerevisiae* iso-1 and horse heart cytochrome *c*

	R_g(Å)[a]
S. cerevisiae iso-1 cytochrome *c*	
folded	14.5
molten globule[b]	18.2
acid unfolded	22
Horse heart cytochrome *c*[c]	
folded	13.5
molten globule	17.4
acid unfolded	24.2

[a]Identical R_gs were observed for DNS(C102)-cyt *c* and C102S variant unless noted
[b]C102S mutant
[c]Kataoka *et al.* , J. Mol. Biol. (1993) 229, 591-596

Fluorescence Decay Kinetics

We have obtained ***D-A*** distance distributions in DNS(C102)-cyt *c* under conditions favoring the molten globule (**Figure 5.7**). At salt concentrations of 100 mM or lower, the polypeptide ensemble is highly heterogeneous: 50% of the polypeptides are in extended conformations with ***D-A*** distances > 35 Å; the remaining 50% are in compact conformations with ***D-A*** distances < 35 Å. As the salt concentration is increased further (100–500 mM), the

fraction of polypeptides in extended conformations decreases in favor of compact structures, but both populations remain heterogeneous. At high salt concentrations (≥ 700 mM), all of the polypeptides are compact with ***D-A*** distances between 25 and 30 Å. The fractional populations (**Figure 5.8**) of compact (r < 35 Å) and extended (r > 35 Å) distributions parallel amplitude changes observed by circular dichroism upon addition of salt, but the FET-probed transition from the acid-denatured state to the molten globule is more prominent. FET kinetics measurements clearly reveal that the populations of compact and extended polypeptides are extremely heterogeneous below 700 mM [Na_2SO_4].

FET kinetics measured during DNS(C102)-cyt *c* folding show that dilution of denaturant to concentrations favoring native protein conformations ([GuHCl] = 0.13 M) do not produce a complete collapse of the polypeptide ensemble.[18] Within the deadtime of stopped-flow measurements, we find that only 40% of the protein population has formed compact structures. The compact ensemble has a mean DNS-heme separation of ~27 Å, which is greater than that of the native protein, indicating that the collapsed molecules are not fully folded. As the population of proteins with the native fold increases, extended and compact polypeptides disappear on comparable timescales. On the basis of these observations as well as on folding measurements on Co-substituted cyt *c*,[32] we conclude that extended and collapsed populations in this folding intermediate are in rapid equilibrium.

The picture is similar in the case of "refolding" the acid denatured protein with added Na_2SO_4. At relatively low salt concentrations ([Na_2SO_4] = 50 mM), both collapsed and extended structures are present at equilibrium. The compact ensemble has a mean DNS-heme separation of ~30 Å and the extended polypeptide population exhibits DNS-heme distances greater than 40 Å. The collapsed structures in the molten globule are reminiscent of the

compact ensemble observed during DNS(C102)-cyt *c* refolding.[18] As the salt concentration is increased, the compact ensemble becomes more compact and shifts to shorter distances (25-30 Å) with concomitant decrease of the population of extended conformations. Thus, at high salt concentrations, the ***D-A*** distances in the collapsed ensemble are virtually indistinguishable from those in the native population.

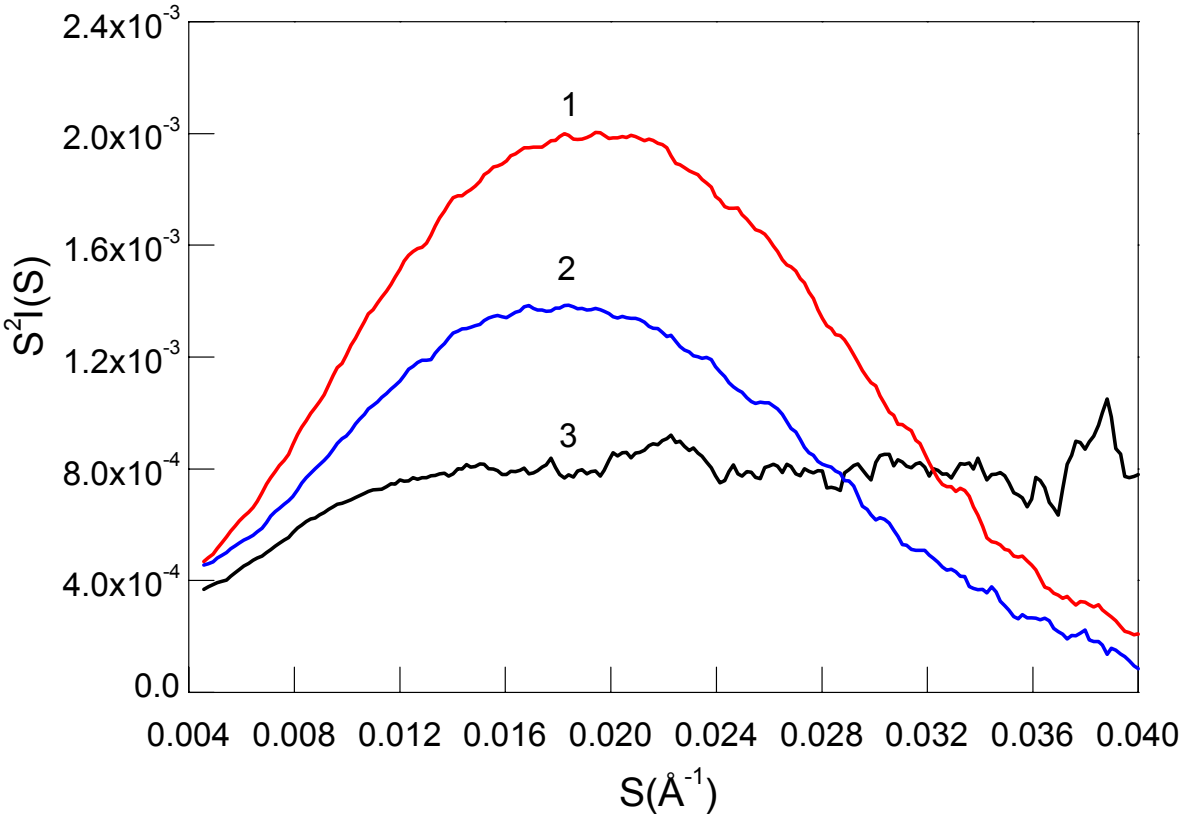

Figure 5.5. Kratky plot, $S^2I(S)$ vs S, of yeast iso-1 cytochrome *c*. (1) native state (NaPi, pH 7, μ 0.1 M); (2) molten globule state (~ 400 mM Na_2SO_4/H_2SO_4, pH 2); and (3) acid unfolded state (H_2SO_4, pH 2).

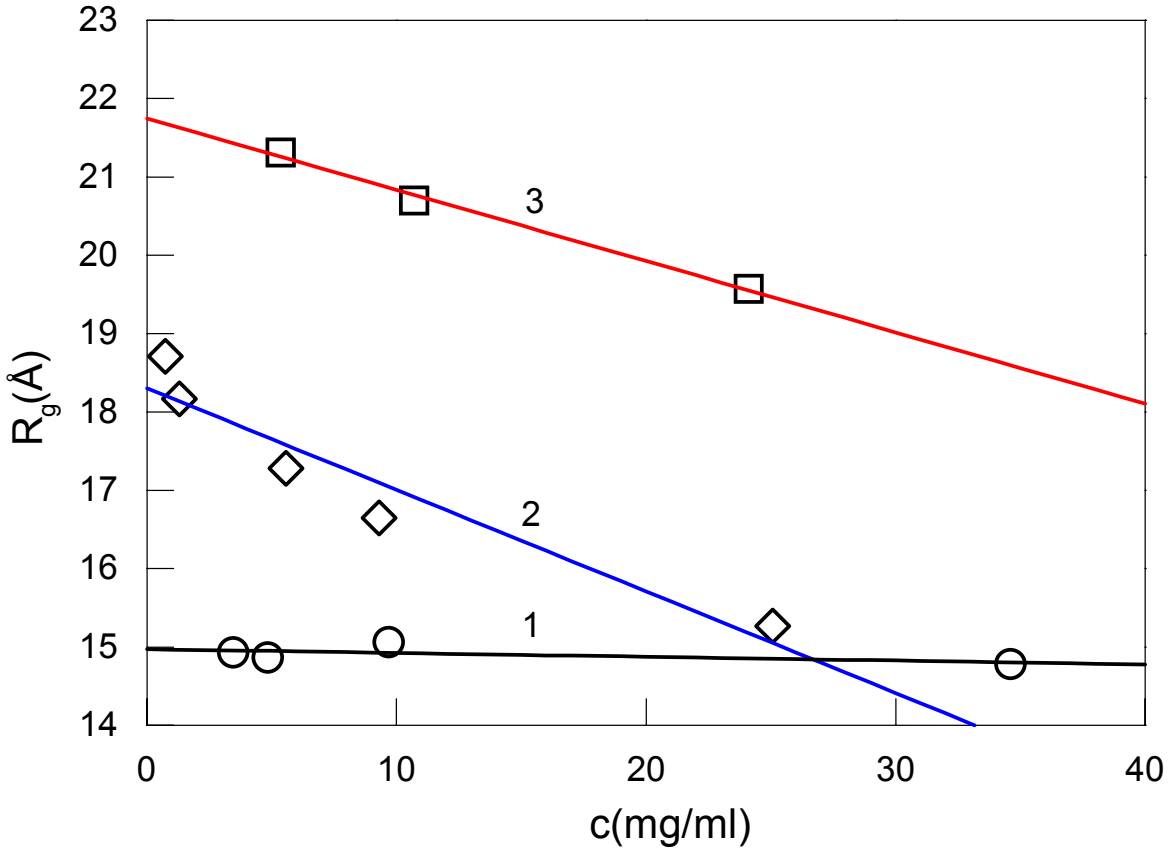

Figure 5.6. Radii of gyration calculated from Guinier plots plotted against the protein concentration for (1) native state (NaPi, pH 7, μ 0.1 M); (2) molten globule state (~ 400 mM Na_2SO_4/H_2SO_4, pH 2); and (3) acid unfolded state (H_2SO_4, pH 2) of yeast iso-1 cytochrome *c*. Lines are extrapolations to zero protein concentrations.

CONCLUSIONS

The structural homogeneity of folded proteins can be disrupted by a variety of chemical and physical perturbations. FET kinetics measurements on DNS(C102)-cyt *c* reveal a large degree of heterogeneity in the acid-denatured protein. High salt concentrations convert the observed complex mixture of conformations into an ensemble of compact (r < 35 Å) polypeptides with a mean ***D-A*** separation quite close to that of the native protein (25 Å). This molten globule is somewhat more compact and far more homogeneous than the ensemble of polypeptides present in the burst intermediate formed during cyt *c* folding.[18,33-36] A clear transition between the acid-denatured and molten globule forms of cyt *c* is not apparent from most ensemble-averaged spectroscopic probes (UV-VIS absorption, CD, fluorescence intensity). FET kinetics, however, provide definitive evidence for the formation of a uniformly compact molten globule at salt concentrations greater than 700 mM. It remains to be determined if polyols, alcohols, and other molten-globule stabilizing agents[37-39] are as effective as anions in shifting the collapsed/extended equilibrium to a position in which compact states are dominant.

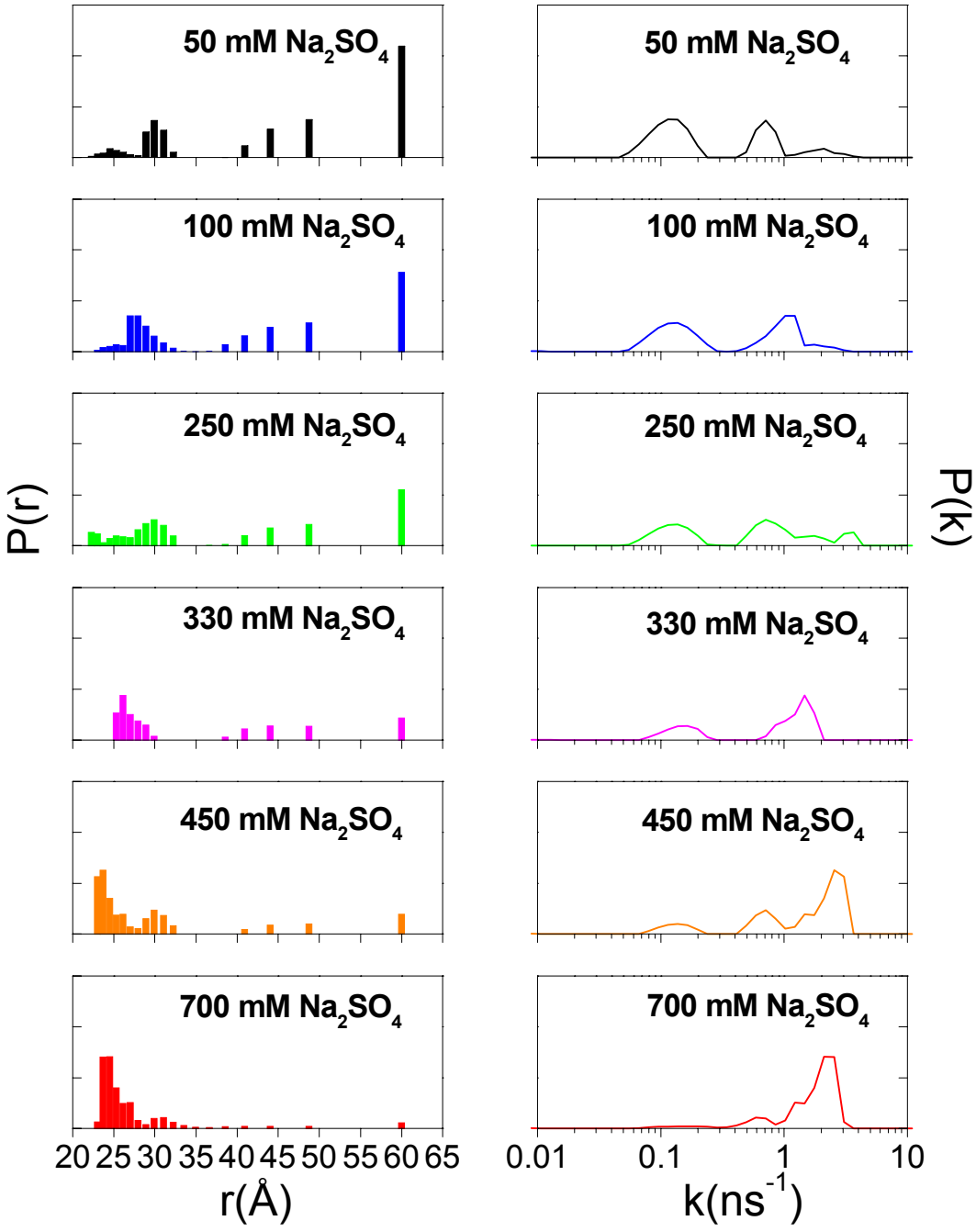

Figure 5.7. Na_2SO_4 induced changes in the distribution of the luminescence decay rates (*P(k)*, right) and ***D-A*** distances (*P(r)*, left) in DNS(C102)-cyt *c* (pH 2, 22°C). Kinetics data fit using ME algorithm.

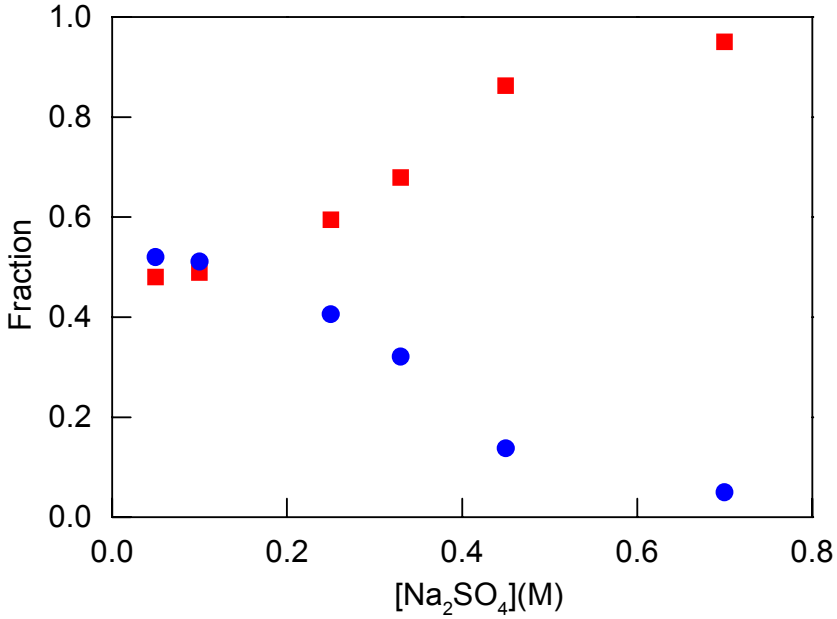

Figure 5.8. Fraction of compact (r < 35 Å, ■) and extended (r >35Å, ●) distributions as a function of Na_2SO_4 concentration.

REFERENCES AND NOTES

(1) Baldwin, R. *Curr. Opin. Struct. Biol.* **1993**, *3*, 84-91.

(2) Ohgushi, M.; Wada, A. *FEBS Lett.* **1983**, *164*, 21-24.

(3) Riddihough, G. *Nat. Struct. Biol.* **1994**, *367*, 98.

(4) Kuwajima, K.; Arai, M. The Molten Globule State: The Physical and Biological Significance. In *Mechanisms of Protein Folding*; 2nd ed.; Pain, R. H., Ed.; Oxford University Press:, 2000; pp 138-174.

(5) Feng, Y.; Sligar, S. G.; Wand, A. J. *Structural Biology* **1994**, *1*, 30-35.

(6) Redfield, C.; Smith, R. A.; Dobson, C. M. *Structural Biology* **1994**, *1*, 23- 29.

(7) Eliezer, D.; Chung, H. J.; Wright, P. E. *Biochemistry* **2000**, *39*, 2894-2901.

(8) Dobson, C. M. *Curr. Opin. Struct. Biol.* **1992**, *2*, 6-12.

(9) Ptitsyn, O. B.; Pain, R. H.; Semisotnov, G. V.; Zerovnik, E.; Razgulyaev, O. I. *FEBS Lett.* **1990**, *262*, 20-24.

(10) Colón, W.; Roder, H. *Nat. Struct. Biol.* **1996**, *3*, 1019-1025.

(11) Goto, Y.; Takahashi, N.; Fink, A. L. *Biochemistry* **1990**, *29*, 3480-3488.

(12) Santucci, R.; Bongiovanni, C.; Mei, G.; Ferri, T.; Polizio, F.; Desideri, A. *Biochemistry* **2000**, *39*, 12632-12638.

(13) Saunders, A. J.; Davis-Searles, P. R.; Allen, D. L.; Pielak, G. J.; Erie, D. A. *Biopolymers* **1999**, *53*, 293-307.

(14) Bychkova, V. E.; Dujsekina, A. E.; Klenin, S. I.; Tiktopulo, E. I.; Uversky, V. N.; Ptitsyn, O. B. *Biochemistry* **1996**, *35*, 6058-6063.

(15) Konno, T.; Iwashita, J.; Nagayama, K. *Protein Science* **2000**, *9*, 564-569.

(16) Navon, A.; Ittah, V.; Landsman, P.; Scheraga, H. A.; Haas, E. *Biochemistry* **2001**, *40*, 105-118.

(17) Lakshmikanth, G. S.; Sridevi, K.; Krishnamoorthy, G.; Udgaonkar, J. B. *Nat. Struct. Biol.* **2001**, *8*, 799-804.

(18) Lyubovitsky, J. G.; Gray, H. B.; Winkler, J. R. *J. Am. Chem. Soc.* **2002**, *124*, 5481-5485.

(19) Wakatsuki, S.; Hodgson, K. O.; Eliezer, D.; Rice, M.; Hubbard, S.; Gillis, N.; Doniach, S. *Rev. Sci. Instrum.* **1992**, *63*, 1736-1740.

(20) Segel, D. J.; Fink, A. L.; Hodgson, K. O.; Doniach, S. *Biochemistry* **1998**, *37*, 12443-12451.

(21) Doniach, S. *Chem. Reviews* **2000**.

(22) Glatter, O.; Kratky, O. *Small Angle X-ray scattering*; Academic Press: New York, 1982.

(23) Myer, Y. P.; Ajay, P. Circular Dichroism Studies of Hemoproteins and Heme Models. In *The Porphyrins*; Academic Press, Inc.:, 1978; Vol. III; pp 271-323.

(24) Goto, Y.; Calciano, L. J.; Fink, A. L. *Proc. Natl. Acad. Sci. USA* **1990**, *87*, 573-577.

(25) Dyson, H. J.; Beattie, J. K. *J. Biol. Chem.* **1982**, *257*, 2267-2273.

(26) Lanir, A.; Aviram, I. *Arch. Biochem. Biophys.* **1975**, *166*, 4439-445.

(27) Lanir, A.; Yu, N. T.; Felton, R. H. *Biochemistry* **1979**, *18*, 1656-1660.

(28) Bren, K. L.; Gray, H. B. *J. Am. Chem. Soc.* **1993**, *115*, 10382-10383.

(29) Aviram, I. *J. Biol. Chem.* **1973**, *248*, 1894-1896.

(30) Marmorino, J. L.; Pielak, G. J. *Biochemistry* **1995**, *34*, 3140-3143.

(31) Kataoka, M., Hagihara, Y., Mihara, K., Goto, Y. *J. Mol. Biol.* **1993**, *229*, 591-596.

(32) Tezcan, F. A.; Findley, W. M.; Crane, B. R.; Ross, S. A.; Lyubovitsky, J. G.; Gray, H. B.; Winkler, J. R. *Proc. Natl. Acad. Sci. USA* **2002**, *99*, 8626-8630.

(33) Akiyama, S.; Takahashi, S.; Kimura, T.; Ishimori, K.; Morishima, I.; Nishikawa, Y.; Fujisawa, T. *Proc. Natl. Acad. Sci. USA* **2002**, *99*, 1329-1334.

(34) Englander, S. W.; Sosnick, T. R.; Mayne, L. C.; Shtilerman, M.; Qi, P. X.; Bai, Y. *Acc. Chem. Res.* **1998**, *31*, 737-744.

(35) Pollack, L.; Tate, M. W.; Darnton, N. C.; Knight, J. B.; Gruner, S. M.;

Eaton, W. A.; Austin, R. H. *Proc. Natl. Acad. Sci. USA* **1999**, *96*, 10115-10117.

(36) Shastry, M. C. R.; Roder, H. *Nat. Struct. Biol.* **1998**, *5*, 385-392.

(37) Rankin, S. E.; Watts, A.; Roder, H.; Pinheiro, T. J. T. *Prot. Science* **1999**, *8*, 381-393.

(38) Vidugris, G. J. A.; Royer, C. A. *Biophys. J.* **1998**, *75*, 463.

(39) Yamasaki, K.; Taniguchi, Y.; Takeda, N.; Nakano, K.; Yamasaki, T.; Kanaya, S.; Oobatake, M. *Biochemistry* **1998**, *37*, 18001.